Bottom-up construction of electrochemically active living filters: from graphene oxide mediated formation of bacterial cables to 3D assembly of hierarchical architectures

Pu Deng[1,2]‡, Weiqin Sheng[1,3]‡, Andrew Xu[1]‡, Yixin Zhang[1], Xiaochuan Dai[1], Richard Vo[1], Huan-Hsuan Hsu[1]*, Xiaocheng Jiang[1]*

[1]*Department of Biomedical Engineering, Tufts University, Medford, Massachusetts 02155, USA*

[2]*Thomas Lord Department of Mechanical Engineering & Materials Science, Duke University, Durham, North Carolina 27705, USA*

[3]*School of Electronic Information, Hangzhou Dianzi University, Hangzhou 310018, People's Republic of China*

ABSTRACT: Living composites comprising of both biotic and abiotic modules are shifting the paradigm of materials science, yet challenges remain in effectively converging their distinctive structural and functional attributes. Here we present a bottom-up hybridization strategy to construct functionally coherent, electrochemically active biohybrids with optimal mass/charge transport, mechanical integrity, and biocatalytic performance. This biohybrid can overcome several key limitations of traditional biocarrier designs and demonstrate superior efficiency in metabolizing low-concentration toxic ions with minimal environmental impact. Overall, this work exemplifies a new bio-integration strategy that complements existing synthetic biology toolsets to further expand the range of material attributes and functionalities.

KEYWORDS: Exoelectrogen, living hybrid materials, 3D assembly, hierarchical structures, bioelectrochemical systems.

Exoelectrogens, microorganisms that are capable of cross-membrane transport of metabolically generated electrons,[1] represent unique living building blocks for the construction of electroactive biosystems. Encoded with a range of extracellular electron transfer (EET) pathways,[2] they have been expanding the spectrum of functional living material designs and empowering applications in bioelectronics,[3] energy,[4] and environmental science.[5] The performance of these living devices to date, however, remains limited by the compromised charge and/or mass transport that is inherent to the native structural assemblies (*i.e.* electroactive biofilms). For example, modeling of *G. sulfurreducens* biofilm grown on planar electrodes indicates that the cells furthest from the electrode barely respire/divide due to their low efficiency to remotely exchange electrons with electrode,[6] while the high diffusion resistance across the native biofilm further limits the access to nutrient/metabolite exchange for inner layers of cells and their electrochemical performance.[7]

Bio-hybridization with complementary material components could potentially overcome these intrinsic limits imposed by biomolecular/cellular building blocks. Through mixing with conductive dopants, such as metal nanoparticles,[8] carbon nanotubes,[9] graphene,[10] or conducting polymers,[11] composite biofilms have been fabricated with increased electrical conductivity and mechanical strength, enabling enhanced power generation,[12] biosynthesis,[13] or wastewater treatment.[14] These physical- or chemical-based hybridization approaches, however, are typically limited by the inefficient structural (poor interfacial contact) and functional (large interfacial charge transfer barrier) integration at the biotic-abiotic junctions. Additionally, the lack of microenvironmental control leads to substantial fluctuation in cell functioning (*e.g.* metabolic rate) over longer length and time scales that further impedes system-level performance.[15]

In comparison, biologically driven hybridization processes, such as bio-mineralization, present unique opportunities for improved cross-system integration by initiating and directing the interplay with foreign components from the bottom up.[16] Bone mineralization, for example, enables highly specific and ordered incorporation of nanocrystalline apatite in the gap regions of self-assembled type I collagen fibrils, leading to hierarchically structured calcified tissues with superior mechanical properties that cannot be matched by synthetic materials. Similarly, exoelectrogens are known for their unique capability to electrically interact with external electron acceptors and in-situ deposit inorganic materials (such as Au, Ag, Pd, and FeS_x nanoparticles) on outer-membranes.[17] These dissimilatory reduction processes actively engage direct electron exchanges with biosynthesis to bridge biological and solid-state charge transport systems at these hybrid interfaces.

Here we report a multiscale hybridization strategy that converges both assembly modalities to generate electrochemically active living materials with enhanced performance. In particular, the living catalysts, *Shewanella loihica* PV-4, are converted into conductive bacterial "cables" through spatially-confined biomineralization, where the metabolic pathways of individual bacterium are electrically conjugated to form expanded EET networks with significantly increased active surface area. These 1D composite building blocks are further engineered into 3D hierarchical frameworks through bio-printing with rationally designed physiochemical characteristics (Figure 1a). As-prepared bio-hybrids have the potential to overcome the inherent limits in mass/charge transport of native bioelectrochemical systems, reinforce a range of applications in energy and environmental science, and broadly impact how functional living materials can be designed and constructed.[18]

At the cellular level, structural and functional integration is initiated with the bio-reduction of graphene oxide (GO), the critical "linker" that is converted into conductive rGO through the metabolism of *S. loihica*. Based on our previous research, GO holding intimate contacts with bacteria can be fully converted to reduced GO as confirmed by Raman spectroscopy.[19] These bio-reduced GO can intimately couple with its outer membrane cytochromes and electrically connecting adjacent cells (Figure 1b). Specifically, bioinks formulated with *S. loihica*, GO and alginate are processed and extruded through a co-axial microfluidic device,[20] where the ionically crosslinked

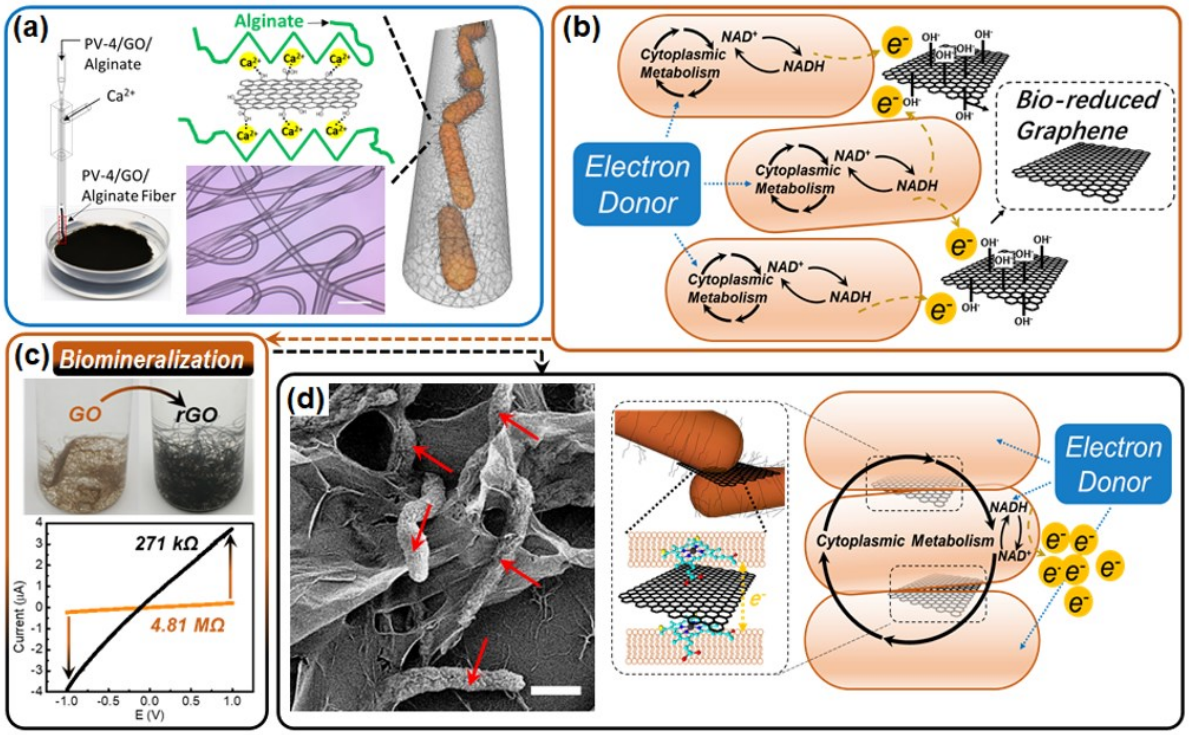

Figure 1. Design, assembly and characterization of the living filter: (a) schematics showing the living filter design at ensemble (3-D assembly of the microfibers) and microscopic (graphene oxide (GO)-cation-alginate interactions) levels; (b) Schematic showing the dissimilatory reduction by alginate encapsulated *S. Ioihica* before biomineralization; (c) Biomineralization/bioreduction of GO, which is evidenced by both the brown-to-black color change (top) and the decrease of electrical resistance of bacterial cables (bottom); (d) Schematic and SEM characterization of assembled/biomineralized cell network (scale bar: 300 nm), of which the individual *S. Ioihica* are structurally- and functionally- integrated through the reduced GO enabled cellular assembling.

alginate shell provides porous scaffolding with structural similarity to polysaccharides for 1D cell confinement, while allowing efficient nutrient/metabolite exchange. The bio-transformation of GO into rGO is evidenced by the progressive color change (brown to black) of the hydrogel fibers during a 24-hour culture (Figure 1a) as well as 95% reduction of two-probe resistance (Figure 1c). As-reduced GO represents bio-synthetic electron conduits that actively "wire" the redox center of cytochromes in electroactive conformations and significantly reduces the barrier for interfacial charge transport.[19] This GO-hybridized fiber allows significantly expanding the effective EET active surface area that is critical to many downstream applications (*e.g.* microbial fuel cells and bio-remediation). At the molecular level, the structural integrity of the composite microfibers is further strengthened by the interaction between GO and alginate (Figure 1a), where the carbonyl and hydroxyl groups on GO help confine the crosslinking cations within the alginate matrices.[21] The chronic stability of the biohybrid is significantly improved, which remains intact and robust after > 48 hours, while alginate/*S. loihica* fibers without GO becomes fragile due to the degradation/dissociation of the cross-linked alginate and weaker cell-cell interconnections (Figure S1 & S2). As a result, mechanically reinforced and electrochemically coherent bacterial networks can be formed (Figure 1d and SEM insert).

The hierarchical structural/functional integration at larger scales is achieved through spatially-organized assembly of these 1D hybrid building blocks *via* bioprinting. A customized, extrusion-based bioprinter (Figure S3) with a multi-inlet microfluidic nozzle is developed, where factors defining individual fibers (diameter and composition) and their 3D placement (pitch/porosity) can be programmed (Figure S4&S5). This approach allows the bottom-up engineering of key mass- and charge-transport properties that are critical to many downstream applications. For example, biological water treatment provides an attractive opportunity in effective toxic ion removals, which can eliminate the disadvantages of the physical and chemical based treatment techniques.[12] Recently, many biological species such as algae, bacteria, fungi are studied toward this prospective. Among all these species, the unique EET process allows EABs to directly reduce the highly toxic soluble inorganic ions (i.e. Chromium,[22] Arsenic,[23] Cadmium,[24] etc.) toward solid-state low-toxicity nanoparticles. Additionally, since wastewater is abundant in organic matters as the electron donors, EABs are self-sustainable in this environment and have demonstrated extraordinary possibilities in electricity recovery during water treatments.[25] Hence, EABs offer exclusive possibilities in the development of next generation low cost, low energy consumption and self-sustainable wastewater treatment strategies.[26] As a proof of concept, we demonstrate the design and application of this 3-D biocatalyst network as a "living filter" for bio-remediation, which converge the advantages of existing treatment options, *i.e.*, (a) biocarriers (low biomass contamination but compromised mass/charge transport); and (b) planktonic bacteria (high treatment efficiency but requiring onerous post-treatment). Their performance is systematically evaluated in simulated wastewater treatments along with their bulk- or planktonic- counterparts for the reduction of hexavalent chromium (Cr(VI)), one of the most common sources of water

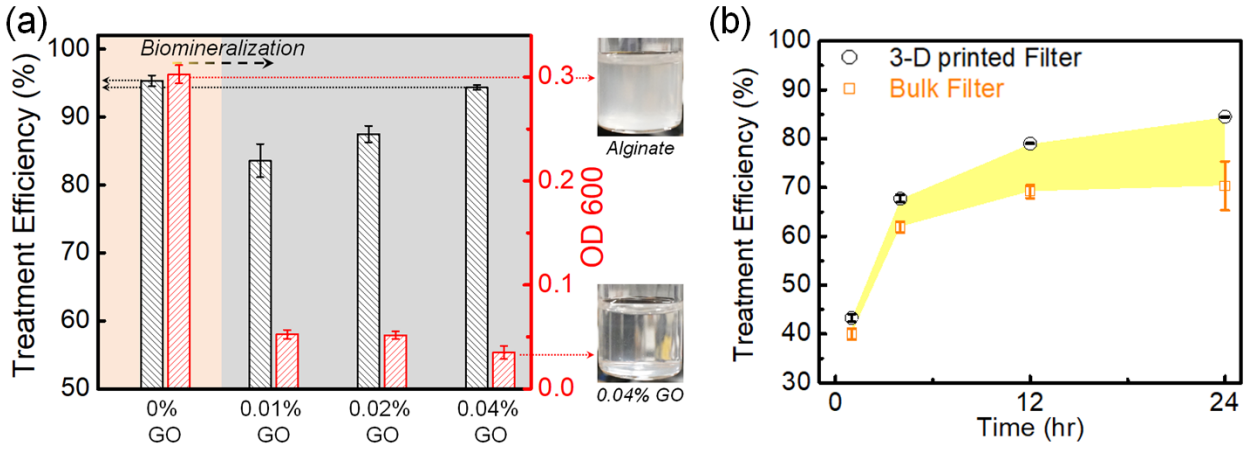

Figure 2. Chronic stability and performance of living filters with different compositions and macro-structures: (a) Cr(VI) treatment efficiency and planktonic/leaked *S. loihica* level (OD600, red bars) of filters made of 5 mL bioink with different GO contents. The high efficiency of filter made of pure alginate (0% GO) is mainly attributed to the planktonic *S. loihica*; (an insert) Images of treated water with high (0.3) and low (0.03) OD600; (b) Cr(VI) treatment efficiencies of mesh (60% macro-porosity) versus solid (0% macro-porosity) filters made of 2 mL bioink. Yellow area indicates the difference in treatment efficiency between two types of filters (n = 3).

contaminants in U.S.[22]. The procedures of simulated wastewater treatments are detailed in support information. The initial concentration of Cr^{6+} (190 μM) were selected based on previous research [doi:10.1128/AEM.02463-10]

The incorporation and biomineralization with GO are found to play important roles in improving the structural integrity and treatment efficiency of the living filters. As shown in Figure 2a, the OD-600 (red bars, correspondent to the planktonic *S. loihica*) of the post-treatment solution by filters made of pure alginate can reach 0.3 after 24 hours, almost 20% of the fed-batch (planktonic) culture in the stationary phase (1.5-2.2). This result indicates that the native bacteria/alginate composites are prone to dissociate and leak, particularly with the mesh design, as a result of its significantly increased surface area/decreased alginate thickness when compared with conventional biocarriers. However, biomineralization can reinforce the intercellular connections by "gluing" adjacent *S.loihica* with rGO to improve chronic stability. Together with the interactions between alginate and GO that stabilize the crosslinks of alginate molecules, the OD-600 can be maintained at below 0.07 during the treatment with GO-doped living filters (Figure 2a). Overall, these results demonstrate significantly improved mechanical integrity and chronic stability of living filters with the incorporation of GO linkers, hence minimal biomass production/post-processing, which remains one of the major challenges in biological water treatment.

The hybridization with GO also enhances the overall treatment efficiency by improving the system-level EET (Figure 2). The treatment efficiency of Cr(VI) is determined by a EPA approved standard method detailed in support information. As shown, the reduction of Cr(VI) is positively correlated with the increase of GO concentration, and reaches 92% at GO 0.02%. This increased biocatalytic kinetics can be attributed to the rGO mediated electrical interconnection between encapsulated *S. loihica*, which substantially expands the active EET area beyond the outer membranes of individual bacterium (Figure 1d). Although filters made of pure alginate show a higher removal rates at 96%, this is mainly contributed by the leaked planktonic *S. loihica* (OD 600 = 0.3 as compared with 0.03 for GO doped filters, Figure 2a inset), which are immediately accessible to nutrients/Cr(VI) and metabolically more active. In GO-doped living filters, despite the mass transport barrier imposed by the alginate/GO matrix (to maintain minimal bacteria leakage), the Cr(VI) removal remains competitively efficient as a result of improved charge and mass transport compared with traditional biocarriers. Overall, the experiments demonstrated that bio-reduced GO is critical in the biohybrid network, which not only maintain the biocatalytic/electron transport efficiency toward the comparable level as planktonic bacteria (which are much more mass transport favorable), but also maintain the long-term structural integrity to avoid the bacteria leakage. Besides, the bio-reduced GO enhanced structural integrity provides additional possibility for the recycle/reusage of living filter toward the life span of *S. loihica*.[27] While further increasing GO may provide additional benefit for treatment efficiency enhancement, the higher GO content can also challenge the printability (forming aggregates that could block the printing nozzle) and long-term stability (incompatibility of hydrophobic rGO with alginate hydrogel that leads to brittle fibers) of living filter.[28]

To further evaluate the effect of filter structure on mass transport and Cr(VI) reduction, we compare the performance of assembled mesh filter (60% macro-porosity) with its bulk counterpart (0% macro-porosity) made of identical components (Figure 2b) (SI Methods). The difference in treatment efficiency between the two filter designs is highlighted in yellow. Rapid Cr(VI) conversion can be achieved by both mesh- (68 %) and bulk- (62 %) filters within the first 4-hour, when the initial high concentration gradient of Cr(VI) drives efficient inward diffusion. Cr(VI) treatment by bulk filter plateaus after 12 hours when diffusion becomes a limiting factor (Cr(VI) at ~ 67 μM, ~65% treated). In contrast, the Cr(VI) treatment steadily increases with mesh filter design until the experiments are terminated at 24 hours. The 24-hour duration is selected while the amont/effect of planktonic *S. loihica* remain negligible (OD600 = 0.03). The enhanced mass transport can be attributed to the thin fiber diameter (~23 μm) and hierarchically assembled 3D

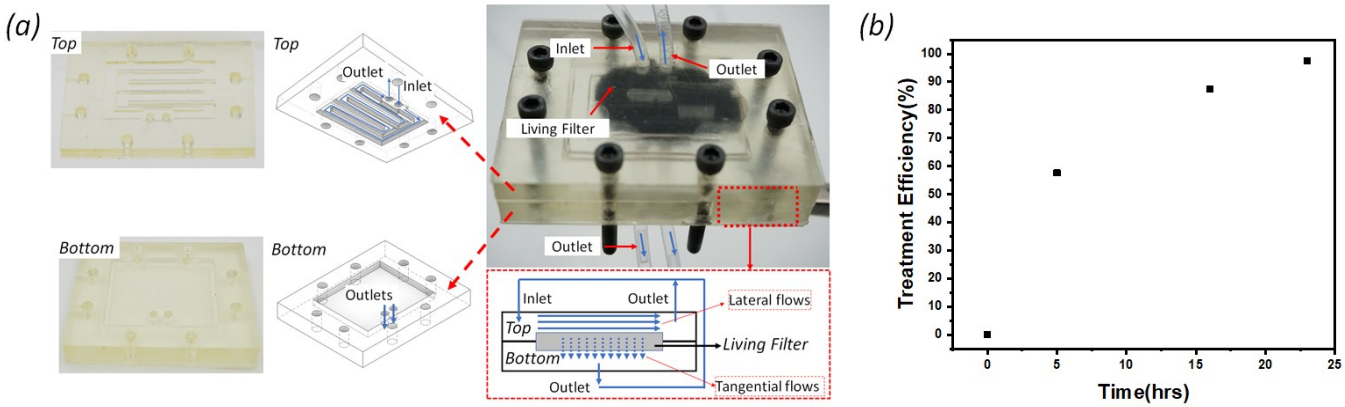

Figure 3. Living filter performance under continuous flow setting: (a) images and schemes of the bioreactor. In the reactor, the top layer was the flow channel that introduced both lateral and tangential flows to the living filter, the middle layer was the living filter and the bottom layer was the reservoir for collecting the tangential flow to be delivered back to main reservoir; and (b) the 24-hour Cr(VI) treatment efficiency of the living filter inside the bioreactor.

porous structure, which becomes critically important in overcoming the diffusion limit in bulk alginate (pore size ~5 nm, diffusion coefficient 4.10×10^{-6} cm^2/min), especially when the concentration gradient is low.[29,30]

The structural integrity and mechanical stability of free-standing living filters could significantly reduce the cost and energy consumption associated with the integration, maintenance, and post-treatment of the biocatalysts. The design is also fully compatible with existing wastewater treatment infrastructure for sustainable operation. In particular, we have designed a semi-continuous flow bioreactor in which both lateral and tangential flows can be programmed to maximize the flow-filter interaction while reducing the direct hydrodynamic impacts (**Method** & Figure 3). In the test, Cr(VI) conversion rate was significantly increased (60% at 4 hours, and 100% at 24 hrs) as compared with the results from batch processing (Figure 2a & 3), demonstrating the potential of dynamic flow programming to further circumvent native mass transport limits at low concentration regimes.

In summary, we demonstrate a multi-modality, bottom-up assembling strategy to generate electrochemically active living filters with seamless structural and functional integration, of which, assembled *S. loihica* networks have demonstrated their unique biocatalytic ability for Cr(VI) removal while their efficiency and chronic stability are enhanced significantly through the GO-assisted assembling processes. At the cellular level, the biomineralization/hybridization with GO inside hydrogel fibers leads to improved EET and strengthened inter-cellular/molecular interactions that eventually benefit the mechanical stability and performance enhancement. At the macroscopic level, these biohybrid cables are hierarchically assembled into a 3-D biocatalytic network that largely overcomes the mass transport limit in traditional biocarrier design. Moving forward, the design and implementation of electrochemically active biohybrids will add another important dimension to the existing library of functional living materials, and open up extensive opportunities in accomplishing widely-defined tasks (*e.g.* catalyst, synthesis, sensing, remediation, computing) with unique dynamic attributes including self-regulation, environmental responsiveness, and sustainability.

ASSOCIATED CONTENT

Supporting Information.
This material is available free of charge via the Internet at http://pubs.acs.org.
Materials and methods. Additional data S1-S6 (PDF)

AUTHOR INFORMATION

Corresponding Author

*Huan-Hsuan. Hsu- Department of Biomedical Engineering, Tufts University, Medford, MA 02155, United States; https://orcid.org/0000-0001-9455-6816; Email: Huan-Hsuan.Hsu@tufts.edu.

*Xiaocheng Jiang- Department of Biomedical Engineering, Tufts University, Medford, MA 02155, United States; https://orcid.org/0000-0002-3455-3653; Email: Xiaocheng.Jiang@tufts.edu.

Authors

Pu Deng- Department of Biomedical Engineering, Tufts University, Medford, MA 02155, United States;

Thomas Lord Department of Mechanical Engineering & Materials Science, Duke University, Durham, North Carolina 27705, USA; https://orcid.org/0000-0001-5190-5350

Weiqin Sheng- Department of Biomedical Engineering, Tufts University, Medford, MA 02155, United States

School of Electronic Information, Hangzhou Dianzi University, Hangzhou 310018, People's Republic of China

Andrew Xu- Department of Biomedical Engineering, Tufts University, Medford, MA 02155, United States

Yixin Zhang- Department of Biomedical Engineering, Tufts University, Medford, MA 02155, United States

Xiaochuan Dai- Department of Biomedical Engineering, Tufts University, Medford, MA 02155, United States

Richard Vo- Department of Biomedical Engineering, Tufts University, Medford, MA 02155, United States

Author Contributions

‡ P. D., W. S., and A. X. contributed equally to this work

Notes

The authors declare no competing financial interest.

ACKNOWLEDGMENT

The authors gratefully acknowledge support from National Science Foundation (NSF DMR-1652095), Tufts Faculty Research Award and TUBERS Program.

REFERENCES

(1) Logan, B. E.; Rossi, R.; Ragab, A.; Saikaly, P. E. Electroactive Microorganisms in Bioelectrochemical Systems. *Nat. Rev. Microbiol.* **2019**, *17* (May), 307–319. https://doi.org/10.1038/s41579-019-0173-x.

(2) Lovley, D. R. Electrically Conductive Pili: Biological Function and Potential Applications in Electronics. *Curr. Opin. Electrochem.* **2017**, *4* (1), 190–198. https://doi.org/10.1016/j.coelec.2017.08.015.

(3) Zhang, Y.; Hsu, L. H.-H.; Jiang, X. Living Electronics. *Nano Res.* **2019**, *12* (1), 22–26. https://doi.org/10.1007/s12274-019-2570-x.

(4) Logan, B. E. Exoelectrogenic Bacteria That Power Microbial Fuel Cells. *Nat. Rev. Microbiol.* **2009**, *7* (5), 375–381. https://doi.org/10.1038/nrmicro2113.

(5) Biological, G.; Lovley, D. R. E-Biologics: Fabrication of Sustainable Electronics with "Green" Biological Materials. *Am. Soc. Microbiol.* **2017**, *8* (3), 1–7.

(6) Bonanni, P. S.; Bradley, D. F.; Schrott, G. D.; Busalmen, J. P. Limitations for Current Production in Geobacter Sulfurreducens Biofilms. *ChemSusChem* **2013**, *6* (4), 711–720. https://doi.org/10.1002/cssc.201200671.

(7) Sun, D.; Chen, J.; Huang, H.; Liu, W.; Ye, Y.; Cheng, S. The Effect of Biofilm Thickness on Electrochemical Activity of Geobacter Sulfurreducens. *Int. J. Hydrogen Energy* **2016**, *41* (37), 16523–16528. https://doi.org/10.1016/j.ijhydene.2016.04.163.

(8) Zhang, T.; Nie, H.; Bain, T. S.; Lu, H.; Cui, M.; Snoeyenbos-West, O. L.; Franks, A. E.; Nevin, K. P.; Russell, T. P.; Lovley, D. R. Improved Cathode Materials for Microbial Electrosynthesis. *Energy Environ. Sci.* **2013**, *6* (1), 217–224. https://doi.org/10.1039/c2ee23350a.

(9) Xie, X.; Hu, L.; Pasta, M.; Wells, G. F.; Kong, D.; Criddle, C. S.; Cui, Y. Three-Dimensional Carbon Nanotube-Textile Anode for High-Performance Microbial Fuel Cells. *Nano Lett.* **2011**, *11* (1), 291–296. https://doi.org/10.1021/nl103905t.

(10) Wang, G.; Qian, F.; Saltikov, C. W.; Jiao, Y.; Li, Y. Microbial Reduction of Graphene Oxide by Shewanella. *Nano Res.* **2011**, *4* (6), 563–570. https://doi.org/10.1007/s12274-011-0112-2.

(11) Ding, C.; Liu, H.; Zhu, Y.; Wan, M.; Jiang, L. Control of Bacterial Extracellular Electron Transfer by a Solid-State Mediator of Polyaniline Nanowire Arrays. *Energy Environ. Sci.* **2012**, *5* (9), 8517. https://doi.org/10.1039/c2ee22269h.

(12) Hsu, L. (Huan-H.; Deng, P.; Zhang, Y.; Nguyen, H. N.; Jiang, X. Nanostructured Interfaces for Probing and Facilitating Extracellular Electron Transfer. *J. Mater. Chem. B* **2018**. https://doi.org/10.1039/C8TB01598H.

(13) Kornienko, N.; Zhang, J. Z.; Sakimoto, K. K.; Yang, P.; Reisner, E. Interfacing Nature's Catalytic Machinery with Synthetic Materials for Semi-Artificial Photosynthesis. *Nat. Nanotechnol.* **2018**, *13* (10), 890–899. https://doi.org/10.1038/s41565-018-0251-7.

(14) Zhang, P.; Liu, J.; Qu, Y.; Zhang, J.; Zhong, Y.; Feng, Y. Enhanced Performance of Microbial Fuel Cell with a Bacteria/Multi-Walled Carbon Nanotube Hybrid Biofilm. *J. Power Sources* **2017**, *361*, 318–325. https://doi.org/10.1016/j.jpowsour.2017.06.069.

(15) Wimpenny, J.; Manz, W.; Szewzyk, U. Heterogeneity in Biofilms. **2000**, *24*, 661–671.

(16) Nudelman, F.; Sommerdijk, N. A. J. M. Biomineralization as an Inspiration for Materials Chemistry. *Angew. Chemie - Int. Ed.* **2012**, *51* (27), 6582–6596. https://doi.org/10.1002/anie.201106715.

(17) Narayanan, K. B.; Sakthivel, N. Biological Synthesis of Metal Nanoparticles by Microbes. *Adv. Colloid Interface Sci.* **2010**, *156* (1–2), 1–13. https://doi.org/10.1016/j.cis.2010.02.001.

(18) Nguyen, P. Q.; Courchesne, N. M. D.; Duraj-Thatte, A.; Praveschotinunt, P.; Joshi, N. S. Engineered Living Materials: Prospects and Challenges for Using Biological Systems to Direct the Assembly of Smart Materials. *Adv. Mater.* **2018**, *30* (19), 1–34. https://doi.org/10.1002/adma.201704847.

(19) Hsu, L. H.-H.; Zhang, Y.; Deng, P.; Dai, X.; Jiang, X. Biosynthetic Electronic Interfaces for Bridging Microbial and Inorganic Electron Transport. *Nano Lett.* **2019**, *19*, 8787–8792. https://doi.org/10.1021/acs.nanolett.9b03573.

(20) Hsu, L.; Deng, P.; Zhang, Y.; Jiang, X. Core/Shell Bacterial Cables: A One-Dimensional Platform for Probing Microbial Electron Transfer. *Nano Lett.* **2018**, *18* (7), 4606–4610. https://doi.org/10.1021/acs.nanolett.8b01908.

(21) Valentin, T. M.; Landauer, A. K.; Morales, L. C.; DuBois, E. M.; Shukla, S.; Liu, M.; Stephens Valentin, L. H.; Franck, C.; Chen, P.-Y.; Wong, I. Y. Alginate-Graphene Oxide Hydrogels with Enhanced Ionic Tunability and Chemomechanical Stability for Light-Directed 3D Printing. *Carbon N. Y.* **2019**, *143*, 447–456. https://doi.org/https://doi.org/10.1016/j.carbon.2018.11.006.

(22) Belchik, S. M.; Kennedy, D. W.; Dohnalkova, A. C.; Wang, Y.; Sevinc, P. C.; Wu, H.; Lin, Y.; Lu, H. P.; Fredrickson, J. K.; Shi, L. Extracellular Reduction of Hexavalent Chromium by Cytochromes MtrC and OmcA of Shewanella Oneidensis MR-1. *Appl. Environ. Microbiol.* **2011**, *77* (12), 4035–4041. https://doi.org/10.1128/AEM.02463-10.

(23) Stolz, J. F.; Oremland, R. S. Bacterial Respiration of Arsenic and Selenium. *FEMS Microbiol. Rev.* **1999**, *23* (5), 615–627. https://doi.org/10.1111/j.1574-6976.1999.tb00416.x.

(24) Edberg, S. C.; Rice, E. W.; Karlin, R. J.; Allen, M. J. Escherichia Coli: The Best Biological Drinking Water Indicator for Public Health Protection. *J. Appl. Microbiol.* **2000**, *88* (S1), 106S-116S. https://doi.org/10.1111/j.1365-2672.2000.tb05338.x.

(25) Logan, B. E.; Rabaey, K. Conversion of Wastes into Bioelectricity and Chemicals by Using Microbial Electrochemical Technologies. *Science (80-.).* **2012**, *337* (6095), 686–690. https://doi.org/10.1126/science.1217412.

(26) Logan, B. E.; Hamelers, B.; Rozendal, R.; Schröder, U.; Keller, J.; Freguia, S.; Aelterman, P.; Verstraete, W.; Rabaey, K. Microbial Fuel Cells: Methodology and Technology. *Environ. Sci. Technol.* **2006**, *40* (17), 5181–5192. https://doi.org/10.1021/es0605016.

(27) Yan, F. F.; Wu, C.; Cheng, Y. Y.; He, Y. R.; Li, W. W.; Yu, H. Q. Carbon Nanotubes Promote Cr(VI) Reduction by Alginate-Immobilized Shewanella Oneidensis MR-1. *Biochem. Eng. J.* **2013**, *77*, 183–189. https://doi.org/10.1016/j.bej.2013.06.009.

(28) Choe, G.; Oh, S.; Seok, J. M.; Park, S. A.; Lee, J. Y. Graphene Oxide/Alginate Composites as Novel Bioinks for Three-Dimensional Mesenchymal Stem Cell Printing and Bone Regeneration Applications. *Nanoscale* **2019**, *11* (48), 23275–23285. https://doi.org/10.1039/c9nr07643c.

(29) Lee, K. Y.; Mooney, D. J. Alginate: Properties and Biomedical Applications. *Prog. Polym. Sci.* **2012**, *37* (1), 106–126. https://doi.org/10.1016/j.progpolymsci.2011.06.003.

(30) Tanaka, H.; Matsumura, M.; Veliky, I. A. Diffusion Characteristics of Substrates in Ca-alginate Gel Beads. *Biotechnol. Bioeng.* **1984**, *26* (1), 53–58. https://doi.org/10.1002/bit.260260111.

For table of contents only

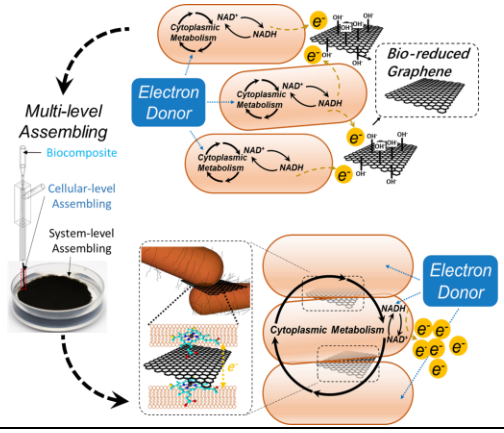
Multi-level Assembling
Biocomposite
Cellular-level Assembling
System-level Assembling
Electron Donor
Bio-reduced Graphene
Cytoplasmic Metabolism
NAD+
NADH
e-
OH
Electron Donor
Cytoplasmic Metabolism
NADH
NAD+